Gate-controlled spin-spin interactions in lateral quantum dot molecules

Yun-Pil Shim and Pawel Hawrylak
Quantum Theory Group, Institute for Microstructural Sciences, National Research Council of Canada, Ottawa, Ontario, Canada K1A 0R6

(Received 25 June 2008; revised manuscript received 18 August 2008; published 20 October 2008)

We present a method of changing the effective spin-spin interactions of electrons localized in quantum dot molecules from antiferromagnetic to ferromagnetic using electrical means. We show that starting with antiferromagnetic interaction of two electrons localized in two quantum dots, the effective spin-spin interaction can change to ferromagnetic by allowing interaction with a third dot containing two spin singlet electrons. The total spin of this four-electron complex can be tuned by changing the third dot potential from singlet to triplet. This is demonstrated using the linear combination of harmonic orbitals combined with the configuration-interaction method mapped onto the Hubbard and an effective *t*-*J* model for the triple dot system. All three approaches predict singlet-triplet spin transition, i.e., a mechanism for changing the magnitude and sign of the effective Heisenberg interaction between two localized spins.

DOI: 10.1103/PhysRevB.78.165317 PACS number(s): 73.21.La, 03.67.Lx

I. INTRODUCTION

Manipulating the spin-spin interactions of localized spins is essential for the realization of spintronic and quantum information devices.[1–5] Lateral quantum dots (QD) defined in two-dimensional electron systems by surface gate electrodes are particularly interesting due to their tunability by applied gate voltages and scalability. Lateral gates allow for the localization of a controlled number of electrons.[6] In ideal single dots, the one-electron energy levels are given by the Fock-Darwin (FD) states, with the resulting shell structure.[5] The total spin of QDs with few electrons is determined by generalized Hund's rule.[7,8] In practice, gate anisotropy and disorder prevent the formation of spin-polarized complexes. The spin states of electrons in a single QD can however be tuned by the magnetic field or by the gate voltages at a fixed magnetic field.[9] In double quantum dots (DQDs), tunneling and exchange interactions lead to complex molecular spin states.[10–14] For dots with one electron each, coherent manipulation of the spin states was demonstrated using external and nuclear magnetic fields.[15,16] As expected, the interaction of the spins of the two electrons was antiferromagnetic; since in the absence of a magnetic field, the two electrons in an arbitrary confining potential always have spin singlet ground state.

In this work we discuss a method of changing the effective spin-spin interaction. We show that starting with antiferromagnetic interaction of two electrons localized in two quantum dots, the effective spin-spin interaction can change to ferromagnetic. This ferromagnetic interaction arises by coupling the two electrons to a third dot containing two spin singlet electrons. Hence the total spin of the two-electron complex can be tuned from singlet to triplet by changing the potential of the third dot. The spin properties of a resonant triple quantum dot (TQD) molecule and, in particular, the existence of a spin-polarized complex of four electrons have been discussed already.[17–20] Recently, the tunability of the number of electrons and their spatial distribution in a lateral TQD system was experimentally demonstrated,[21–23] with transport experiments in a magnetic field showing coherent coupling between the dots.[24,25]

In a resonant TQD with four electrons, the ground state is predicted to be a spin triplet.[17] Surprisingly, the singlet-triplet gap of the four-electron complex is predicted to be proportional to the tunneling matrix element *t*: a single electron property. This cancellation of electron-electron interactions was understood as a result of the nontrivial interplay of statistics and topology of a TQD molecule. It was also shown that the magnetic field through the Aharonov-Bohm effect allows engineering of the degeneracy of the molecular orbitals,[19,20] leading to singlet-triplet transitions with increasing magnetic field.

In this paper, we present a purely electrical method of generating the singlet-triplet transition in the ground state of a TQD molecule with four electrons. We consider a TQD with triangular geometry as shown schematically in Fig. 1. We start with two quantum dots (dots 1 and 3) containing one electron each; a part of a larger quantum dot network. A third dot (dot 2) is energetically well separated from the other two dots. With dots 1 and 3 on resonance, the spin-spin interaction is antiferromagnetic. We next change the bias of dot 2 containing two electrons; one with spin up and the other with spin down. We show that the interaction of the two localized electrons in dots 1 and 3 changes sign at a

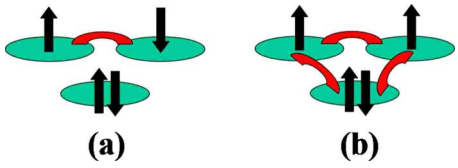

FIG. 1. (Color online) Schematic diagram of a four-electron spin complex of a TQD system in triangular geometry. Two dots contain a single electron each and a third dot contains two spin-singlet electrons. (a) When the dot containing two singlet electrons are energetically well separated from the other dots, the system is essentially a two-electron spin complex. The interaction between the two localized spins is antiferromagnetic. (b) We can change the gate voltage to bring the dot with two electrons energetically closer to the other two dots with localized electrons. The interaction between two localized electrons changes from antiferromagnetic to ferromagnetic.

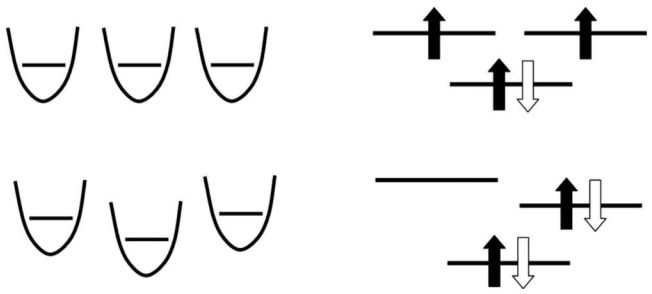

FIG. 2. Total spin transition induced by biasing one of the dots. The energy levels on the left are the single electron energy levels of the three isolated QDs and the energy levels on the right are of the molecular orbitals of the TQD. At resonant case, the doubly degenerate excited molecular levels are occupied by electrons with same spin directions due to the exchange interaction. If a bias is applied to one of the dots, the degeneracy is lifted. With strong enough bias the two lowest molecular levels are both doubly occupied, resulting in spin singlet ground state.

critical value of the bias of dot 2 without significant delocalization of the two active electrons. As the third dot is brought into resonance, the ground state remains triplet but the pair of spin-polarized electrons is delocalized among the three quantum dots. This triplet-singlet transition can be understood in terms of the degeneracy of the molecular orbitals which is controlled by biasing one of the dots, as schematically depicted in Fig. 2.

The plan of this paper is as follows. In Sec. II we introduce three different methods for describing the electronic properties of a TQD molecule. In Sec. II A, we use the harmonic orbitals of each quantum dot as basis states and describe how we can construct molecular orbitals as linear combinations of harmonic orbitals (LCHO). In Sec. II B, the Hubbard model is derived from the LCHO method by repeatedly using perturbation theory described in Appendix A. Both LCHO method and Hubbard Hamiltonian are combined with the configuration-interaction (CI) method to determine the ground and excited states of the TQD system. In Sec. II C, we derive an effective *t-J* Hamiltonian in a reduced Hilbert space of the Hubbard Hamiltonian. This effective *t-J* Hamiltonian gives a more intuitive picture of the spin properties of the system. In Sec. III, we present our numerical results. Using LCHO-CI method we show that near the singlet-triplet spin transition the biased dot is filled with two electrons and the other two dots are singly occupied. It is shown that the spin transition is due to the change of the spin state of two localized spins. The Hubbard model and the *t-J* model are shown to well describe the essential physics of the spin transition. In Sec. IV, we give a brief summary of results.

II. METHODS

A. Linear combination of harmonic orbitals

In this paper, all the energies are expressed in unit of the effective Rydberg $\mathcal{R}=m_e^* e^4/2\epsilon^2\hbar^2$ and all lengths in unit of the effective Bohr radius $a_B=\epsilon\hbar^2/m_e^* e^2$. m_e^* is the effective mass of the electron, e is the electron charge, and ϵ is the dielectric constant. With GaAs parameters $m_e^*=0.067m_0$ and $\epsilon=12.4$, we have $\mathcal{R}=5.93$ meV and $a_B=9.79$ nm. A single electron in a triple quantum dot system depicted in Fig. 1 is described by the Hamiltonian

$$\hat{H}_{\mathrm{SP}} = -\nabla^2 + \sum_{i=1}^{3} V_i(\mathbf{r}), \tag{1}$$

where we assume that the confining potential $V_i(\mathbf{r})$'s have a Gaussian form $V_i(\mathbf{r})=-V_{i,0}\exp[-(\frac{\mathbf{r}-\mathbf{r}_i}{d_i})^2]$ centered around the position of the ith dot $\mathbf{r}_i$ located at vertices of an equilateral triangle. The Gaussian potential is separated into the harmonic part $V_i^{\mathrm{HO}}(\mathbf{r})$ and the anharmonic part $\delta V_i(\mathbf{r})$,

$$V_i(\mathbf{r}) = -V_{i,0} + \frac{\Omega_i^2}{4}(\mathbf{r}-\mathbf{r}_i)^2 + \delta V_i(\mathbf{r}) \equiv V_i^{\mathrm{HO}}(\mathbf{r}) + \delta V_i(\mathbf{r}), \tag{2}$$

where $\Omega_i=2\sqrt{V_{i,0}}/d_i$ is the characteristic energy of the harmonic confinement. Following the method developed in our previous work,[19] we expand the wave function in terms of harmonic-oscillator orbitals localized on each quantum dot and obtain a generalized eigenvalue problem for expansion coefficients $\mathbf{a}$,

$$\mathbf{H}_{\mathrm{SP}}\mathbf{a} = \varepsilon\mathbf{S}\mathbf{a}, \tag{3}$$

where $\mathbf{S}$ is the overlap matrix resulting from the nonorthogonality of the harmonic orbitals from different quantum dots and $\mathbf{a}$ is the eigenvector. This can be cast into a standard eigenvalue problem

$$\mathbf{H}'_{\mathrm{SP}}\mathbf{b} = \varepsilon\mathbf{b}, \tag{4}$$

where $\mathbf{H}'_{\mathrm{SP}}=(\sqrt{\mathbf{S}})^{-1}\mathbf{H}_{\mathrm{SP}}\sqrt{\mathbf{S}}$ and $\mathbf{b}=\sqrt{\mathbf{S}}\mathbf{a}$. $\sqrt{\mathbf{S}}$ is found to be $\mathbf{V}_S\mathbf{E}_S^{1/2}\mathbf{V}_S^\dagger$ where $\mathbf{V}_S$ is the eigenvector matrix of $\mathbf{S}$ and $\mathbf{E}_S$ is the diagonal matrix with eigenvalues of $\mathbf{S}$. In this paper, we obtain the molecular orbitals by solving the above single-particle problem using s and p orbitals from each dot. Once we obtain the molecular orbitals, the many-body Hamiltonian is given by

$$\hat{H} = \sum_{\lambda\sigma} \varepsilon_\lambda c_{\lambda\sigma}^\dagger c_{\lambda\sigma} + \frac{1}{2}\sum_{\lambda_1\lambda_2\lambda_3\lambda_4}\sum_{\sigma\sigma'} \langle\lambda_1\lambda_2|\hat{V}_C|\lambda_3\lambda_4\rangle c_{\lambda_1\sigma}^\dagger c_{\lambda_2\sigma'}^\dagger c_{\lambda_3\sigma'} c_{\lambda_4\sigma}, \tag{5}$$

where λ's are indices for the molecular orbitals, σ is the spin, and

$$\langle\lambda_1\lambda_2|\hat{V}_C|\lambda_3\lambda_4\rangle = \int d\mathbf{r}\int d\mathbf{r}'\,\psi_{\lambda_1}^*(\mathbf{r})\psi_{\lambda_2}^*(\mathbf{r}')\frac{2}{|\mathbf{r}-\mathbf{r}'|} \times \psi_{\lambda_3}(\mathbf{r}')\psi_{\lambda_4}(\mathbf{r}) \tag{6}$$

is the Coulomb matrix element in the molecular-orbital basis. To solve the many-body problem, we take all possible configurations as our basis for many-electron states and exactly diagonalize the resulting many-body Hamiltonian matrix.

B. Hubbard model

Since electrons are well localized in each quantum dot, we can use the Hubbard Hamiltonian to model the system. In this section, we will explicitly derive the Hubbard Hamiltonian from the LCHO method. If we include only *s* orbitals from each dot, the diagonal and off-diagonal elements of $\mathbf{H}'_{\mathrm{SP}}$ in Eq. (4) correspond to the on-site energy and tunneling elements in the Hubbard model, respectively. If we include more than one harmonic orbital from each dot and the energy differences between the higher orbitals and the *s* orbitals are much larger than the off-diagonal elements, we can derive the Hubbard Hamiltonian containing only one orbital from each dot by using the partitioning perturbation theory described in Appendix A. We separate the single electron Hilbert space into subspaces $\mathbb{D}_A$ and $\mathbb{D}_B$, such that $\mathbb{D}_A$ is spanned by *s* orbitals from each dot and $\mathbb{D}_B$ is spanned by all the other harmonic orbitals. We transform the Hamiltonian to a block-diagonal form to separate the subspaces $\mathbb{D}_A$ and $\mathbb{D}_B$ using the first-order perturbation theory iteratively. The first-order approximation of the unitary operator $\hat{U} \simeq 1+\hat{S}^{(1)} \equiv \hat{U}_1$ transforms Eq. (4) into $\mathbf{H}_1\mathbf{b}_1=\varepsilon\mathbf{S}_1\mathbf{b}_1$, where $\mathbf{H}_1=\mathbf{U}_1^{\dagger}\mathbf{H}'_{\mathrm{SP}}\mathbf{U}_1$, $\mathbf{b}_1=\mathbf{U}_1^{-1}\mathbf{b}$, and $\mathbf{S}_1=\mathbf{U}_1^{\dagger}\mathbf{U}_1$. The matrix elements of $\hat{S}^{(1)}$ which makes $\mathbf{H}_1$ block diagonal up to first order are given in Eqs. (A5) and (A6). Note that $\hat{U}_1$ is not precisely unitary and therefore we have nontrivial overlap matrix $\mathbf{S}_1$ in the transformed eigenvalue equation. This is a generalized eigenvalue problem as in the LCHO method and we can transform this into a standard eigenvalue problem,

$$\mathbf{H}'_1\mathbf{b}'_1 = \varepsilon\mathbf{b}'_1. \tag{7}$$

The transformed matrix $\mathbf{H}'_1$ is not exactly block diagonal but the off-diagonal blocks are of the second order because the off-diagonal blocks of $\mathbf{H}_1$ are of the second order and the deviation of $\mathbf{S}_1$ from the identity matrix is also of the second order. Now we can perform the same procedures of the first-order partitioning perturbation theory and the orthonormalization of the basis iteratively, until it reaches the desired accuracy. The resulting Hamiltonian matrix represents the system in the basis of new orbitals which are orthogonal to each other and still well localized in each dot. The diagonal elements are the on-site energy of each localized levels and the off-diagonal elements are the tunneling matrix elements in the Hubbard Hamiltonian.

Combining the direct Coulomb interaction between the localized orbitals obtained in this way, the Hubbard Hamiltonian is given by

$$\hat{H}_{\mathrm{Hubbard}} = \sum_{i,\sigma} \varepsilon_i c_{i\sigma}^{\dagger} c_{i\sigma} + \sum_{i\neq j}\sum_{\sigma} t_{ij} c_{i\sigma}^{\dagger} c_{j\sigma} + \sum_i U_i \hat{n}_{i\uparrow}\hat{n}_{i\downarrow} + \frac{1}{2}\sum_{i\neq j} V_{ij}\hat{\rho}_i\hat{\rho}_j, \tag{8}$$

where $\hat{n}_{i\sigma}=c_{i\sigma}^{\dagger}c_{i\sigma}$ and $\hat{\rho}_i=\hat{n}_{i\uparrow}+\hat{n}_{i\downarrow}$ and $i,j=1,2,3$ are indices for each quantum dot and $\sigma=\pm$ is the spin. The first term ($\equiv\hat{H}_0$) is the kinetic energy, the second term ($\equiv\hat{T}$) is the tunneling between different dots, the third term ($\equiv\hat{H}_U$) is the on-site Coulomb repulsion, and the last term ($\equiv\hat{H}_V$) is the direct Coulomb interaction between two particles in different dots (see Fig. 3). The first two terms are obtained by the iterative transformation described above and the Coulomb interaction *U*'s and *V*'s are obtained by directly calculating the Coulomb matrix elements in the new localized orbital basis obtained after all the transformations. This Hubbard Hamiltonian can be solved using configuration-interaction method as in the LCHO-CI method.

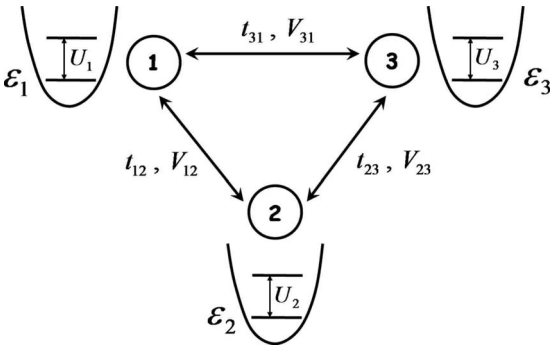

FIG. 3. Parameters of the Hubbard Hamiltonian of a TQD system. ε_i is the energy level of the *i*th QD and t_{ij} is the tunneling matrix element between dots *i* and *j*. U_i is the on-site Coulomb repulsion in dot *i* and V_{ij} is the direct Coulomb interaction between two electrons in dots *i* and *j*.

C. *t-J* Hamiltonian

For a four-electron system in a TQD, it is easier to work in the hole picture rather than the electron picture. A hole is defined as the absence of an electron with respect to the completely filled configuration with six electrons. Thus, a four-electron system corresponds to a two-hole system. The particle-hole transformation in the Hubbard Hamiltonian corresponds to the changes $t_{ij}\rightarrow -t_{ij}^{*}$ and $\varepsilon_i \rightarrow -\varepsilon_i - U_i - 2\Sigma_{j(\neq i)}V_{ij}$. Thus lowering the confining potential of dot 2 corresponds to increasing the hole orbital energy of dot 2. In the following, all the operators and parameters are for holes. Note that in the hole picture, the tunneling matrix elements t_{ij}'s are real and positive, in contrast to the electron picture where the tunneling elements are real and negative. For half-filled systems with three electrons (or three holes), the Hubbard Hamiltonian can be reduced to a Heisenberg spin Hamiltonian.[26,27] But for two-hole systems, it reduces to an effective *t-J* Hamiltonian in a reduced Hilbert space formed by low-energy configurations. We define two subspaces of two-hole Hilbert space according to the number of doubly occupied dots. $\mathbb{D}_A$ consists of configurations with no doubly occupied dot, and $\mathbb{D}_B$ consists of configurations with a dot doubly occupied by two holes (see Fig. 4). We make use of the partitioning perturbation theory in Appendix A to find effective Hamiltonian of subspace $\mathbb{D}_A$ (see Appendix B for explicit derivation). Introducing the spin operators

$$\mathbf{S}^{(i)} \equiv \frac{1}{2}\sum_{\alpha\beta} c_{i\alpha}^{\dagger}\boldsymbol{\sigma}_{\alpha\beta}c_{i\beta}, \tag{9}$$

where $\boldsymbol{\sigma}$ is the vector of Pauli matrices, the effective *t-J* Hamiltonian restricted in subspace $\mathbb{D}_A$ is

FIG. 4. Possible configurations of the TQD system with two holes. The circles represent holes and the separation between two levels in the same dot is the on-site Coulomb repulsion energy U. Configurations with no doubly occupied dot belong to $\mathbb{D}_A$ and configurations with a doubly occupied dot belong to $\mathbb{D}_B$. The energy levels of the second dot are shifted by Δ by applying appropriate voltages to the gate electrodes. Configurations in $\mathbb{D}_B$ have much higher energy than configurations in $\mathbb{D}_A$ due to the large on-site Coulomb repulsion energy.

$$\hat{H}_{t\text{-}J} = \hat{H}_0 + \hat{H}_U + \hat{H}_V + \hat{T} + \hat{H}_J + \hat{H}_3, \tag{10}$$

where

$$\hat{H}_J = \sum_{\langle i,j\rangle} J_{ij}\left(\mathbf{S}^{(i)} \cdot \mathbf{S}^{(j)} - \frac{1}{4}\hat{n}_i\hat{n}_j\right), \tag{11}$$

$$\hat{H}_3 = \sum_{i\neq j\neq l(\neq i)} J_{ijl} \sum_{\sigma} (c^{\dagger}_{i\sigma}\hat{n}_{j\bar{\sigma}}c_{l\sigma} - c^{\dagger}_{i\sigma}c^{\dagger}_{j\bar{\sigma}}c_{j\sigma}c_{l\bar{\sigma}}), \tag{12}$$

and $\langle i,j\rangle$ are pairs of different sites i and j, and $\bar{\sigma}$ is the opposite of σ. The coefficients $J_{i,j}$ and J_{ijl} are given in Eqs. (B8)–(B11) for a simple case with $\varepsilon_1=\varepsilon_3=\varepsilon_0$, $\varepsilon_2=\varepsilon_0+\Delta$, $t_{12}=t_{23}=t_{31}=t$, $U_1=U_2=U_3=U$, and $V_{12}=V_{23}=V_{31}=V$, with Δ being the energy shift of the second dot due to the change of the gate voltage.

Since $\hat{H}_{t\text{-}J}$ commutes with the total spin, we can solve the t-J Hamiltonian for spin triplet and spin singlet separately. For spin triplet it is sufficient to consider only one of the three different values of S^z_{tot}. For $S^z_{\text{tot}}=1$, we have three configurations $|T_1\rangle=c^{\dagger}_{3\uparrow}c^{\dagger}_{1\uparrow}|0\rangle$, $|T_2\rangle=c^{\dagger}_{1\uparrow}c^{\dagger}_{2\uparrow}|0\rangle$, and $|T_3\rangle=c^{\dagger}_{2\uparrow}c^{\dagger}_{3\uparrow}|0\rangle$, where $|0\rangle$ is the hole vacuum state. Then the Hamiltonian matrix for the triplet is

$$[\mathbf{H}_{t\text{-}J}]_T = \begin{pmatrix} E_1 & -t & -t \\ -t & E_2 & -t \\ -t & -t & E_2 \end{pmatrix}, \tag{13}$$

where $E_1=2\varepsilon_0+V$ and $E_2=2\varepsilon_0+V+\Delta$. We obtain three triplet eigenvalues and the ground-state energy is

$$E_T = \frac{1}{2}(E_1+E_2-t) - \frac{1}{2}\sqrt{(E_2-E_1-t)^2+8t^2}. \tag{14}$$

For the spin singlet, we have three configurations $|S_1\rangle=\frac{1}{\sqrt{2}}(c^{\dagger}_{3\uparrow}c^{\dagger}_{1\downarrow}+c^{\dagger}_{1\uparrow}c^{\dagger}_{3\downarrow})|0\rangle$, $|S_2\rangle=\frac{1}{\sqrt{2}}(c^{\dagger}_{1\uparrow}c^{\dagger}_{2\downarrow}+c^{\dagger}_{2\uparrow}c^{\dagger}_{1\downarrow})|0\rangle$, and $|S_3\rangle=\frac{1}{\sqrt{2}}(c^{\dagger}_{2\uparrow}c^{\dagger}_{3\downarrow}+c^{\dagger}_{3\uparrow}c^{\dagger}_{2\downarrow})|0\rangle$. The Hamiltonian matrix for the singlet is

$$[\mathbf{H}_{t\text{-}J}]_S = \begin{pmatrix} \tilde{E}_{A_1} & \tilde{t} & \tilde{t} \\ \tilde{t} & \tilde{E}_{A_2} & \tilde{t}' \\ \tilde{t} & \tilde{t}' & \tilde{E}_{A_2} \end{pmatrix}, \tag{15}$$

where

$$\tilde{E}_1 = E_1 - J' = 2\varepsilon_0 + V - \frac{4t^2}{U-V}, \tag{16}$$

$$\tilde{E}_2 = E_2 - J = 2\varepsilon_0 + V + \Delta - 2t^2\left(\frac{1}{U-V-\Delta} + \frac{1}{U-V+\Delta}\right), \tag{17}$$

$$\tilde{t} = t + 2J_3 = t - t^2\left(\frac{1}{U-V} + \frac{1}{U-V-\Delta}\right), \tag{18}$$

$$\tilde{t}' = t + 2J_3' = t - \frac{2t^2}{U-V+\Delta}. \tag{19}$$

The singlet ground-state energy is given by

$$E_S = \frac{1}{2}(\tilde{E}_1+\tilde{E}_2+\tilde{t}') - \frac{1}{2}\sqrt{(\tilde{E}_2-\tilde{E}_1+\tilde{t}')^2+8\tilde{t}^2}. \tag{20}$$

From the Hamiltonian matrices corresponding to the spin triplet and singlet cases [Eqs. (13) and (15)], we can understand the physical meaning of each terms in $\hat{H}_{t\text{-}J}$. Since we are working in the hole picture, the tunneling matrix element t is positive and therefore the tunneling Hamiltonian $\hat{T}$ favors spin triplet configurations. On the other hand, the antiferromagnetic Heisenberg term $\hat{H}_J$ given by Eq. (11) favors the spin singlet configuration. $\hat{H}_3$ defined in Eq. (12), which is usually neglected in the t-J model of high-T_c superconducting materials for small dopings,[28,29] slightly reduces the effective tunneling elements for singlet configurations.

For the case $\Delta=0$, which corresponds to a resonant TQD molecule, we obtain

$$E_S - E_T = t - \frac{2t^2}{U-V}. \tag{21}$$

This agrees with the result of Ref. 17. Since t is positive and $t/(U-V)\ll 1$, we have a triplet ground state and the gap between the singlet excited state and the triplet ground state is proportional to the tunneling t. For $t\ll\Delta\ll U$, we have

$$E_S - E_T = -\frac{4t^2}{U-V}. \tag{22}$$

The singlet ground state is separated from the triplet excited state by the usual singlet-triplet gap of DQD systems. In this limit, the second dot is energetically well separated from the other two dots and the two holes in dots 1 and 3 are effectively described by the Heisenberg Hamiltonian $\hat{H}_J$.

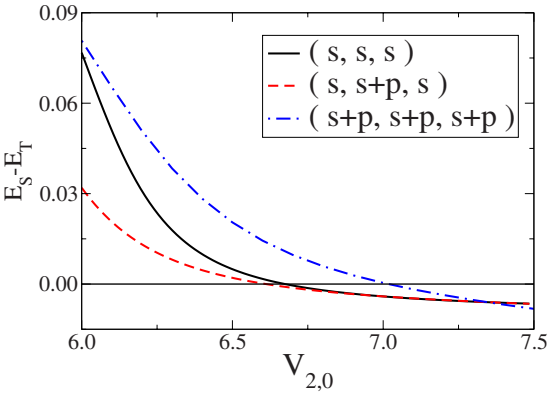

FIG. 5. (Color online) Energy differences between singlet and triplet ground states as a function of the bias $V_{2,0}$ on dot 2 calculated using LCHO-CI method with different numbers of basis harmonic-oscillator states. Solid black curve is with *s* orbitals from each dot, dashed red curve is with *s* orbitals from dots 1 and 3 and *s* and *p* orbitals from dot 2, and dot-dashed blue curve is with *s* and *p* orbitals from each dot. The Gaussian confining potentials are defined by $V_{1,0}=V_{3,0}=6.0$ and $\Omega_1=\Omega_2=\Omega_3=2.5$. The distance between any two dots is 3.7. We changed $V_{2,0}$ from 6.0 to 7.5.

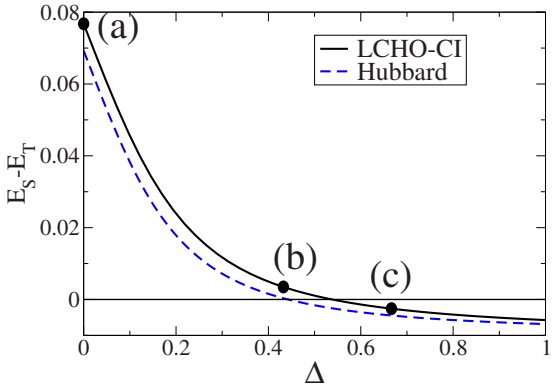

FIG. 6. (Color online) Energy differences between singlet and triplet ground states as a function of the energy shift Δ calculated using LCHO-CI method with only *s* orbitals from each dot(solid curve) and using the Hubbard Hamiltonian with parameters obtained from LCHO-CI method.

III. RESULTS

Now we present the results of numerical calculations for the triangular TQD with four electrons using different methods described in Secs. II A–II C. Figure 5 shows the singlet-triplet spin transition in the ground state obtained by LCHO-CI method with different numbers of harmonic-oscillator orbital basis states. The black solid curve was calculated using only *s* orbitals from each QD. We lowered the Gaussian confining potential of the second dot by increasing $V_{2,0}$ while keeping Ω_2 fixed. As $V_{2,0}$ increases, the energy gap between the triplet and singlet states decreases. At high enough $V_{2,0}$, a spin transition occurs and the ground state becomes spin singlet. The red dashed curve was calculated with *s* orbitals from dots 1 and 3 and *s* and *p* orbitals from dot 2. This is a valid approximation for a moderately high bias $V_{2,0}$ where the *p* orbitals of dots 1 and 3 are energetically higher than the orbitals included. The *p* orbitals of dot 2 are not occupied in the range of $V_{2,0}$ values we consider, and the result is very similar to the result obtained with only *s* orbitals. If *s* and *p* orbitals from all three QDs are included (the blue dot-dashed curve), the effective tunneling between the dots is increased and the spin transition occurs at higher $V_{2,0}$. Although inclusion of higher orbitals would make the spin transition to occur at even higher $V_{2,0}$, the LCHO-CI method with small number of orbitals is accurate enough to describe the essential physics of the spin transition.

Figure 6 compares the results obtained by LCHO-CI (the black solid curve) and the Hubbard Hamiltonian (the blue dashed curve). We used only *s* orbitals from each dot for the LCHO-CI method. The parameters of the Hubbard Hamiltonian are obtained as described in Sec. II B. The *x* axis is the energy shift in the on-site energy of dot 2 induced by changing $V_{2,0}$, and the *y* axis is the energy difference between the singlet and triplet ground states. Initially, in a resonant TQD, the ground state is spin triplet and the gap between the spin singlet and triplet is proportional to the tunneling element *t*. As we lower the energy of dot 2, the gap shrinks and spin singlet becomes the ground state. The slight shift to the left of the Hubbard model result can be accounted for by omitted Coulomb interaction terms in the Hubbard model. The Hubbard Hamiltonian includes only direct Coulomb interactions between localized electrons, while the full Coulomb interaction in the LCHO-CI method includes the exchange interaction which stabilized the spin triplet ground state. Therefore the singlet-triplet transition occurs at higher-energy shift Δ in the LCHO-CI method.

Figure 7 shows how the electron charge density and the *z* component of the spin density change as we apply bias to dot 2 in the LCHO-CI calculation with *s* orbitals from each dot. The charge and spin densities are obtained by calculating the expectation values of the charge and spin-density operators

$$\hat{\rho}(\mathbf{r}) = \sum_{\sigma} \hat{\psi}_{\sigma}^{\dagger}(\mathbf{r})\hat{\psi}_{\sigma}(\mathbf{r}), \tag{23}$$

$$\hat{\mathbf{s}}(\mathbf{r}) = \sum_{\alpha\beta} \frac{1}{2}\hat{\psi}_{\alpha}^{\dagger}(\mathbf{r})\sigma_{\alpha\beta}\hat{\psi}_{\beta}(\mathbf{r}), \tag{24}$$

in the ground state, where $\hat{\psi}_{\sigma}^{\dagger}(\mathbf{r})$ and $\hat{\psi}_{\sigma}(\mathbf{r})$ are the field operators. The upper figures of Fig. 7 show the charge densities

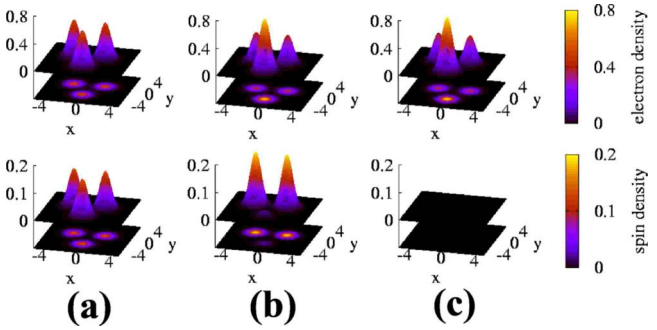

FIG. 7. (Color online) Electron density and *z* component of the spin density of the ground state at three different values of Δ in Fig. 6. The upper (lower) figures show the electron (spin) densities. We choose $S_{\mathrm{tot}}^{z}=1$ for triplet ground states.

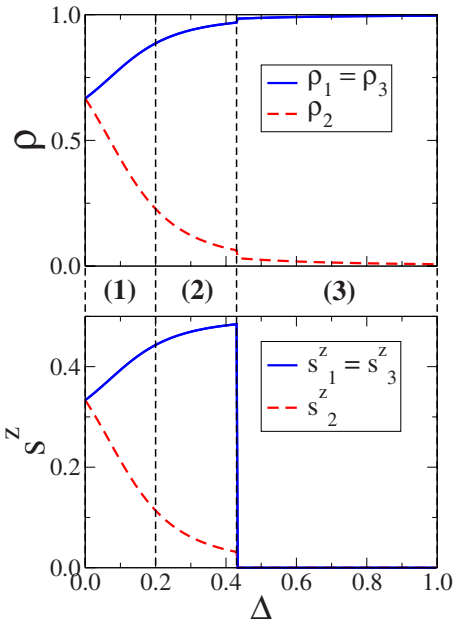

FIG. 8. (Color online) Number of holes (ρ_i: upper panel) and spin (s_i^z: lower panel) of each dot for the ground state as a function of the energy shift Δ calculated using the Hubbard model. Blue curves correspond to the hole number and spin in dots 1 and 3 and red curves correspond to the hole number and spin in dot 2.

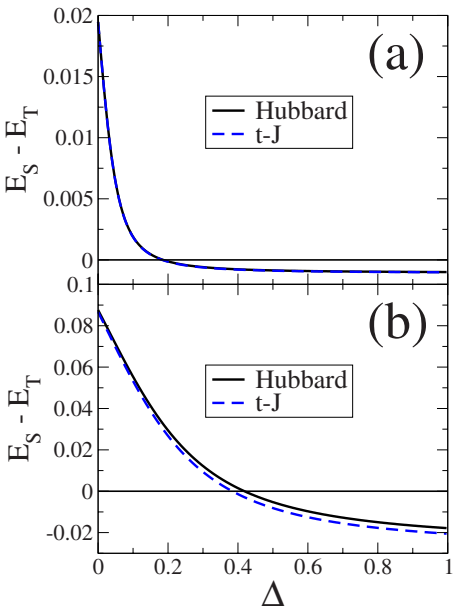

FIG. 9. (Color online) Energy differences between singlet and triplet ground states as a function of the energy shift Δ calculated using the Hubbard model (black solid curve) and the effective t-J model (blue dashed curve). (a) is for $t=0.02$ and (b) is for $t=0.1$. $U=2.0$ and $V=0.5$ for both (a) and (b). Antiferromagnetic-ferromagnetic transition occurs at $\Delta_0=0.18$ for (a) and 0.42 for (b).

and the lower figures the z components of the spin densities for three different values of Δ shown in Fig. 6. For the spin triplet ground states, we chose $S^z_{\text{tot}}=1$. In a resonant TQD molecule [Fig. 7(a)], the ground state is a spin triplet and is a linear combination of three configurations (2,1,1), (1,2,1), and (1,1,2). Each quantum dot has one electron and the extra electron can be in any of the three dots with the same probability. As we lower the energy of the second dot [Fig. 7(b)], two electrons reside in dot 2 and one electron in dots 1 and 3, respectively. The two electrons in dot 2 have opposite spin directions due to the exclusion principle, thus giving a very low spin density. The other two electrons in dots 1 and 3 have parallel spin directions. So the ground state can be understood as a spin singlet in dot 2 plus two parallel localized spins in dots 1 and 3. For the spin-singlet ground state [Fig. 7(c)], the charge distribution differs very little from case (b). But the two electrons in dots 1 and 3 form spin singlet, therefore they do not contribute to spin density. Similarly, Fig. 8 shows the hole numbers ρ_i and the z component of the spin s_i^z in each dot $i=1,2,3$ as functions of Δ in the Hubbard model. We can consider three different regimes. When the bias Δ is small [region (1)], all three dots are partially occupied by holes. The ground state is a linear combination of configurations with two localized holes. For larger Δ but before the spin transition [region (2)], dot 2 is almost empty of holes and two holes are localized in dots 1 and 3 with parallel spins. The sudden changes in ρ_i and s_i^z at around $\Delta=0.43$ signal the spin singlet-triplet transition in the ground state. At a high enough energy shift Δ [region (3)], the two localized holes form a spin singlet. Therefore Figs. 7 and 8 show that we can control the interaction between two localized spins by the gate voltage in regions (2) and (3).

Figure 9 shows the results obtained by using Hubbard Hamiltonian and t-J Hamiltonian for different tunneling parameters. We used parameters $U=2.0$, $V=0.5$, and $t=0.02$ and 0.1. For the Hubbard Hamiltonian we exactly diagonalized the Hamiltonian matrix in configuration basis, and for the t-J model we compare the triplet and singlet ground-state energies [Eqs. (14) and (20)]. For a small tunneling t [Fig. 9(a)], t-J Hamiltonian gives a very good approximation, while for a large tunneling t [Fig. 9(b)], t-J Hamiltonian gives slightly different results but is still a reasonably good approximation. The gap between singlet and triplet states can be easily tuned by changing t and Δ, which can be accomplished by tuning the gate voltages. As we increase the energy shift Δ, the gap decreases rapidly and the spin state of the ground state changes from triplet to singlet at strong enough bias. After the transition, the change in the gap is relatively small and it approaches the limiting value $-4t^2/(U-V)$. The decrease in E_S-E_T is steeper for smaller t and reaches the limiting value faster because it is easier to satisfy the condition $t \ll \Delta \ll U$ for smaller t. The values of Δ where the transitions occur are much smaller than the on-site Coulomb repulsion U, which is consistent with our initial assumption $U \gg \Delta$.

Figure 10 shows the phase diagram of the total spin as a function of the tunneling t and the energy shift Δ obtained by using the Hubbard model. Since the tunneling Hamiltonian $\hat{T}$ favors the spin triplet, a larger bias is required for the ground state to be a spin singlet as the tunneling t increases.

IV. SUMMARY AND DISCUSSIONS

To summarize, we theoretically demonstrated an electrical method of changing an antiferromagnetic interaction to a fer-

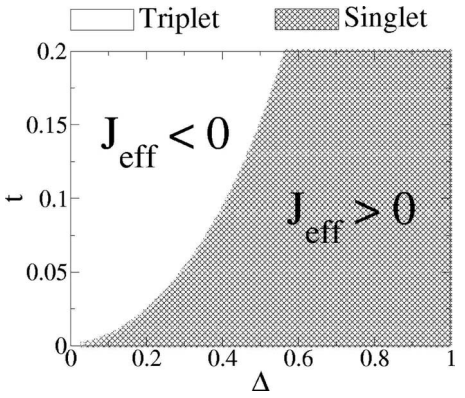

FIG. 10. Phase diagram of singlet and triplet ground states in the space of the energy shift Δ of dot 2 and the tunneling t. White region is for the spin triplet ground state and hashed region is for spin singlet ground state. Spin triplet (singlet) ground state corresponds to negative (positive) effective coupling J_{eff} in the effective Heisenberg Hamiltonian (25).

romagnetic one between two localized electrons in two quantum dots by connecting them with a third dot with two electrons. We explained how to derive the Hubbard Hamiltonian from the microscopic LCHO-CI method using partitioning perturbation theory. In this way we can understand how the external potential can change the Hubbard model parameters in a systematic way. The Hubbard Hamiltonian can also be transformed into an effective t-J Hamiltonian in a restricted Hilbert space. The results show that all three approaches explain the change of the effective interaction and spin transitions between triplet and singlet ground states.

When dot 2 is far from the resonance and the transition point (for a very high Δ), the two electrons in dot 2 are energetically isolated from the electrons in dots 1 and 3. The system then essentially consists of two localized electrons and the ground state is a spin singlet. Near the transition point, dot 2 is still occupied with two electrons and dots 1 and 3 are singly occupied. So the system can be described by an effective Heisenberg Hamiltonian of two localized spins

$$\hat{H}_{\text{eff}} = J_{\text{eff}} \mathbf{S}^{(1)} \cdot \mathbf{S}^{(3)}, \tag{25}$$

and we change the effective interaction from ferromagnetic to antiferromagnetic as well as the magnitude of the coupling constant J_{eff} by tuning the external gate voltages. Controlling the time dependence of J_{eff} by time-dependent gate voltage pulse is of importance in quantum information and computation. Let us take a system prepared to be in the spin singlet ground state, for example. If we decrease J_{eff} so that the change is much slower compared to all decoherence mechanisms present, we can induce the spin singlet-triplet transition. On the other hand if the change in J_{eff} is much faster, then the system will remain a spin singlet. This type of tunability can be useful in realizing spin-based qubits in solid-state systems.

The different spin characters of resonant TQD molecules with two electrons (singlet) and with two holes (triplet) can be also of importance in the context of quantum materials. For example, the two-electron spin singlet states can be considered as a minimal resonating valence bond (RVB) state:[30,31] one of the possible mechanisms of the high-T_c superconductivity. A two-hole triplet state was also predicted in copper compounds with the charge-transfer energy larger than the on-site Coulomb energy.[32] The voltage control of the singlet-triplet transition may open the possibility of inducing ferromagnetic-antiferromagnetic transitions in artificial quantum dot lattices.

ACKNOWLEDGMENTS

The authors thank M. Korkusinski, F. Delgado, A. S. Sachrajda, S. A. Studenikin, and L. Gaudreau for useful discussions. This work is supported by the Canadian Institute for Advanced Research, QuantumWorks, and NRC-CNRS CRP.

APPENDIX A: PARTITIONING PERTURBATION THEORY

In this section, we describe the partitioning perturbation method used to derive an effective Hamiltonian in a restricted Hilbert space. Let us consider a Hamiltonian

$$\hat{H} = \hat{H}_0 + \hat{H}', \tag{A1}$$

where $\hat{H}_0$ is the unperturbed Hamiltonian and $\hat{H}'$ is a small perturbation. We will assume that the eigenstates of $\hat{H}_0$ can be grouped into two subspaces $\mathbb{D}_A$ and $\mathbb{D}_B$, where states in $\mathbb{D}_A$ have similar energies and states in $\mathbb{D}_B$ have much higher energies than states in $\mathbb{D}_A$. The energy difference between states in $\mathbb{D}_A$ and in $\mathbb{D}_B$ is assumed to be much larger than the matrix elements of $\hat{H}'$. The Schrödinger equation for $\hat{H}$ is, in a matrix form,

$$\begin{pmatrix} (\mathbf{H}_0)_{AA} + \mathbf{H}'_{AA} & \mathbf{H}'_{AB} \\ \mathbf{H}'_{BA} & (\mathbf{H}_0)_{BB} + \mathbf{H}'_{BB} \end{pmatrix} \begin{pmatrix} \mathbf{a}_A \\ \mathbf{a}_B \end{pmatrix} = \varepsilon \begin{pmatrix} \mathbf{a}_A \\ \mathbf{a}_B \end{pmatrix}. \tag{A2}$$

We introduce a unitary transformation[28,29,33]

$$\hat{U} = e^{i\hat{S}} = \mathbb{1} + i\hat{S} - \frac{1}{2}\hat{S}^2 - \frac{i}{6}\hat{S}^3 + \cdots, \tag{A3}$$

where $\hat{S}$ is a Hermitian operator, which is assumed to be a sum of terms with different order,

$$\hat{S} = \hat{S}^{(1)} + \hat{S}^{(2)} + \hat{S}^{(3)} + \cdots. \tag{A4}$$

We choose $\hat{S}$ such that the Hamiltonian is block diagonal after transformation by $\hat{U}$ up to a certain order. The matrix elements of the first-order term $\hat{S}^{(1)}$ are given by

$$[\mathbf{S}^{(1)}_{AB}]_{kl} = \frac{i\mathbf{H}'_{kl}}{\varepsilon^{(0)}_k - \varepsilon^{(0)}_l} \quad k \in \mathbb{D}_A, \quad l \in \mathbb{D}_B, \tag{A5}$$

$$[\mathbf{S}^{(1)}_{BA}]_{lk} = \frac{i\mathbf{H}'_{lk}}{\varepsilon^{(0)}_l - \varepsilon^{(0)}_k} \quad k \in \mathbb{D}_A, \quad l \in \mathbb{D}_B, \tag{A6}$$

$$\mathbf{S}^{(1)}_{AA} = \mathbf{S}^{(1)}_{BB} = 0, \tag{A7}$$

and the effective Hamiltonian matrix for the the reduced Hilbert space $\mathbb{D}_A$ up to second order is

$$(\mathbf{H}_{\mathrm{red}})_{AA} = (\mathbf{U}^{\dagger}\mathbf{H}\mathbf{U})_{AA} \simeq (\mathbf{H}_0)_{AA} + \mathbf{H}'_{AA} + \overline{\mathbf{H}}^{(2)}_{AA} = (\mathbf{H}_0)_{AA} + \mathbf{H}'_{AA} + \frac{i}{2}(\mathbf{H}'_{AB}\mathbf{S}^{(1)}_{BA} - \mathbf{S}^{(1)}_{AB}\mathbf{H}'_{BA}). \tag{A8}$$

The last term effectively takes into account the presence of the subspace $\mathbb{D}_B$.

APPENDIX B: DERIVATION OF *t-J* Hamiltonian

In this Appendix, we explicitly derive the *t-J* Hamiltonian [Eq. (10)] for a TQD with two holes from the Hubbard Hamiltonian [Eq. (8)]. The *t-J* Hamiltonian is the effective Hamiltonian restricted to a subspace of lower-energy states. To restrict the Hilbert space to lowest-energy states, we make use of the partitioning perturbation theory in Appendix A. We use all possible configurations as the basis for the many-particle Hubbard Hamiltonian and define the two subspaces as follows: $\mathbb{D}_A$ consists of configurations with no doubly occupied dot and $\mathbb{D}_B$ consists of configurations with a dot doubly occupied by two holes (see Fig. 4). We also assume that $U_i \gg V_{ij}, \Delta, t_{ij}$. The large on-site Coulomb repulsion makes sure that configurations in $\mathbb{D}_B$ have much higher energies than configurations in $\mathbb{D}_A$. $\hat{H}_0$, $\hat{H}_U$, and $\hat{H}_V$ conserve the number of holes at each single hole state, thus diagonal in the configuration basis. The tunneling Hamiltonian $\hat{T}$ can be separated according to whether the tunneling increases or decreases the number of doubly occupied sites,[28,29,33]

$$\begin{aligned}\hat{T} &= \sum_{i\neq j}\sum_{\sigma} t_{ij}c^{\dagger}_{i\sigma}c_{j\sigma} = \sum_{i\neq j}\sum_{\sigma} t_{ij}(\hat{n}_{i\bar{\sigma}} + \hat{h}_{i\bar{\sigma}})c^{\dagger}_{i\sigma}c_{j\sigma}(\hat{n}_{j\bar{\sigma}} + \hat{h}_{j\bar{\sigma}}) \\ &= \sum_{i\neq j}\sum_{\sigma} t_{ij}(\hat{n}_{i\bar{\sigma}}c^{\dagger}_{i\sigma}c_{j\sigma}\hat{n}_{j\bar{\sigma}} + \hat{h}_{i\bar{\sigma}}c^{\dagger}_{i\sigma}c_{j\sigma}\hat{h}_{j\bar{\sigma}}) \\ &\quad + \sum_{i\neq j}\sum_{\sigma} t_{ij}\hat{n}_{i\bar{\sigma}}c^{\dagger}_{i\sigma}c_{j\sigma}\hat{h}_{j\bar{\sigma}} + \sum_{i\neq j}\sum_{\sigma} t_{ij}\hat{h}_{i\bar{\sigma}}c^{\dagger}_{i\sigma}c_{j\sigma}\hat{n}_{j\bar{\sigma}} \\ &\equiv \hat{T}^{(0)} + \hat{T}^{(+)} + \hat{T}^{(-)},\end{aligned} \tag{B1}$$

where $\bar{\sigma}$ is the opposite of σ and $\hat{h}_{i\bar{\sigma}} = 1 - \hat{n}_{i\bar{\sigma}}$. The first term in $\hat{T}^{(0)}$ moves one hole from a doubly occupied site to a singly occupied site, thus conserving the number of doubly occupied sites. The second term in $\hat{T}^{(0)}$ moves one hole from a singly occupied site to an empty site, thus again conserving the number of doubly occupied sites. $\hat{T}^{(+)}$ moves one hole from a singly occupied site to another singly occupied site, increasing the number of doubly occupied sites by one. $\hat{T}^{(-)}$ moves one hole from a doubly occupied site to an empty site, decreasing the number of doubly occupied sites by one. Therefore, $\hat{T}^{(+)}$ and $\hat{T}^{(-)}$ connect the two subspaces $\mathbb{D}_A$ and $\mathbb{D}_B$, while $\hat{T}^{(0)}$ does not. Using Eq. (A8), the effective Hamiltonian matrix in the reduced Hilbert space $\mathbb{D}_A$ is given by

$$\mathbf{H}_{\mathrm{red}} = \mathbf{H}_0 + \mathbf{H}_U + \mathbf{H}_V + \mathbf{T}^{(0)} + \frac{i}{2}[\mathbf{T}^{(-)}_{AB}\mathbf{S}^{(1)}_{BA} - \mathbf{S}^{(1)}_{AB}\mathbf{T}^{(+)}_{BA}], \tag{B2}$$

where the first-order term of $\hat{S}$ is obtained using Eqs. (A5) and (A6),

$$[\mathbf{S}^{(1)}_{AB}]_{kl} = \frac{i[\mathbf{T}^{(-)}_{AB}]_{kl}}{\varepsilon^{(0)}_k - \varepsilon^{(0)}_l} \quad k \in \mathbb{D}_A, \quad l \in \mathbb{D}_B, \tag{B3}$$

$$[\mathbf{S}^{(1)}_{BA}]_{lk} = \frac{i[\mathbf{T}^{(+)}_{BA}]_{lk}}{\varepsilon^{(0)}_l - \varepsilon^{(0)}_k} \quad k \in \mathbb{D}_A, \quad l \in \mathbb{D}_B. \tag{B4}$$

After some algebra, we obtain the effective *t-J* Hamiltonian

$$\hat{H}_{t\text{-}J} = \hat{P}_A[\hat{H}_0 + \hat{H}_U + \hat{H}_V + \hat{T}^{(0)} + \hat{H}_J + \hat{H}_3]\hat{P}_A, \tag{B5}$$

where

$$\hat{H}_J = \sum_{\langle i,j\rangle} J_{ij}\left(\mathbf{S}^{(i)}\cdot\mathbf{S}^{(j)} - \frac{1}{4}\hat{n}_i\hat{n}_j\right), \tag{B6}$$

$$\hat{H}_3 = \sum_{i\neq j\neq l(\neq i)} J_{ijl}\sum_{\sigma}(c^{\dagger}_{i\sigma}\hat{n}_{j\bar{\sigma}}c_{l\sigma} - c^{\dagger}_{i\sigma}c^{\dagger}_{j\bar{\sigma}}c_{j\sigma}c_{l\bar{\sigma}}), \tag{B7}$$

and $\langle i,j\rangle$ are pairs of different sites. $\hat{P}_A$ is the projection operator onto the subspace $\mathbb{D}_A$ and the spin operators are defined in Eq. (9).

For simplicity, we will assume that $\varepsilon_1 = \varepsilon_3 = \varepsilon_0$, $\varepsilon_2 = \varepsilon_0 + \Delta$, $t_{12} = t_{23} = t_{31} = t$, $U_1 = U_2 = U_3 = U$, and $V_{12} = V_{23} = V_{31} = V$, where Δ is the energy shift of the second dot due to the change of the gate voltage. Then J_{ij} and J_{ijk} are given by

$$J_{12} = J_{23} = 2t^2\left(\frac{1}{U - V - \Delta} + \frac{1}{U - V + \Delta}\right) \equiv J, \tag{B8}$$

$$J_{13} = \frac{4t^2}{U - V} \equiv J', \tag{B9}$$

$$J_{ij2} = J_{2jl} = -\frac{t^2}{2}\left(\frac{1}{U - V} + \frac{1}{U - V - \Delta}\right) \equiv J_3, \tag{B10}$$

$$J_{i2l} = -\frac{t^2}{U - V + \Delta} \equiv J'_3. \tag{B11}$$

With the understanding that we use $\hat{H}_{t\text{-}J}$ only in $\mathbb{D}_A$, we can drop the projection operators and noting that

$$\hat{P}_A\hat{T}^{(0)}\hat{P}_A = \hat{P}_A\hat{T}\hat{P}_A, \tag{B12}$$

we obtain the effective *t-J* Hamiltonian

$$\hat{H}_{t\text{-}J} = \hat{H}_0 + \hat{H}_U + \hat{H}_V + \hat{T} + \hat{H}_J + \hat{H}_3. \tag{B13}$$

[1] *Semiconductor Spintronics and Quantum Computation*, Series on Nanoscience and Technology Vol. 16, edited by D. D. Awschalom, D. Loss, and N. Samarth (Springer, New York, 2002).
[2] J. A. Brum and P. Hawrylak, Superlattices Microstruct. **22**, 431 (1997).
[3] D. Loss and D. P. DiVincenzo, Phys. Rev. A **57**, 120 (1998).
[4] D. P. DiVincenzo, D. Bacon, J. Kempe, G. Burkard, and K. B. Whaley, Nature (London) **408**, 339 (2000).
[5] A. S. Sachrajda, P. Hawrylak, and M. Ciorga, in *Electronic Transport in Quantum Dots*, edited by J. P. Bird (Kluwer, Boston, 2003).
[6] M. Ciorga, A. S. Sachrajda, P. Hawrylak, C. Gould, P. Zawadzki, S. Jullian, Y. Feng, and Z. Wasilewski, Phys. Rev. B **61**, R16315 (2000).
[7] A. Wojs and P. Hawrylak, Phys. Rev. B **53**, 10841 (1996).
[8] S. Tarucha, D. G. Austing, T. Honda, R. J. van der Hage, and L. P. Kouwenhoven, Phys. Rev. Lett. **77**, 3613 (1996).
[9] J. Kyriakidis, M. Pioro-Ladriere, M. Ciorga, A. S. Sachrajda, and P. Hawrylak, Phys. Rev. B **66**, 035320 (2002).
[10] J. J. Palacios and P. Hawrylak, Phys. Rev. B **51**, 1769 (1995).
[11] M. Bayer, P. Hawrylak, K. Hinzer, S. Fafard, M. Korkusinski, Z. R. Wasilewski, O. Stern, and A. Forchel, Science **291**, 451 (2001).
[12] M. Pioro-Ladrière, M. Ciorga, J. Lapointe, P. Zawadzki, M. Korkusinski, P. Hawrylak, and A. S. Sachrajda, Phys. Rev. Lett. **91**, 026803 (2003).
[13] M. Pioro-Ladrière, R. Abolfath, P. Zawadzki, J. Lapointe, S. A. Studenikin, A. S. Sachrajda, and P. Hawrylak, Phys. Rev. B **72**, 125307 (2005).
[14] R. M. Abolfath and P. Hawrylak, Phys. Rev. Lett. **97**, 186802 (2006).
[15] J. R. Petta, A. C. Johnson, J. M. Taylor, E. A. Laird, A. Yacoby, M. D. Lukin, C. M. Marcus, M. P. Hanson, and A. C. Gossard, Science **309**, 2180 (2005).
[16] F. H. Koppens, J. A. Folk, J. M. Elzerman, R. Hanson, L. H. W. van Beveren, I. T. Vink, H. P. Tranitz, W. Wegscheider, L. P. Kouwenhoven, and L. M. K. Vandersypen, Science **309**, 1346 (2005).
[17] M. Korkusinski, I. P. Gimenez, P. Hawrylak, L. Gaudreau, S. A. Studenikin, and A. S. Sachrajda, Phys. Rev. B **75**, 115301 (2007).
[18] I. Puerto Gimenez, M. Korkusinski, and P. Hawrylak, Phys. Rev. B **76**, 075336 (2007).
[19] F. Delgado, Y.-P. Shim, M. Korkusinski, and P. Hawrylak, Phys. Rev. B **76**, 115332 (2007).
[20] Y.-P. Shim, F. Delgado, M. Korkusinski, and P. Hawrylak, Physica E (Amsterdam) **40**, 1133 (2008).
[21] L. Gaudreau, S. A. Studenikin, A. S. Sachrajda, P. Zawadzki, A. Kam, J. Lapointe, M. Korkusinski, and P. Hawrylak, Phys. Rev. Lett. **97**, 036807 (2006).
[22] D. Schröer, A. D. Greentree, L. Gaudreau, K. Eberl, L. C. L. Hollenberg, J. P. Kotthaus, and S. Ludwig, Phys. Rev. B **76**, 075306 (2007).
[23] M. C. Rogge and R. J. Haug, Phys. Rev. B **77**, 193306 (2008).
[24] L. Gaudreau, A. S. Sachrajda, S. Studenikin, P. Zawadzki, A. Kam, and J. Lapointe, Proceedings of ICPS Conference, 2006 (unpublished), arXiv:cond-mat/0611488.
[25] T. Ihn, M. Sigrist, K. Ensslin, W. Wegscheider, and M. Reinwald, New J. Phys. **9**, 111 (2007).
[26] V. W. Scarola, K. Park, and S. Das Sarma, Phys. Rev. Lett. **93**, 120503 (2004).
[27] V. W. Scarola and S. Das Sarma, Phys. Rev. A **71**, 032340 (2005).
[28] C. Gros, R. Joynt, and T. M. Rice, Phys. Rev. B **36**, 381 (1987).
[29] A. Paramekanti, M. Randeria, and N. Trivedi, Phys. Rev. B **70**, 054504 (2004).
[30] P. W. Anderson, Science **235**, 1196 (1987).
[31] P. W. Anderson, P. A. Lee, M. Randeria, T. M. Rice, N. Trivedi, and F. C. Zhang, J. Phys.: Condens. Matter **16**, R755 (2004).
[32] H. Eskes and G. A. Sawatzky, Phys. Rev. Lett. **61**, 1415 (1988).
[33] A. H. MacDonald, S. M. Girvin, and D. Yoshioka, Phys. Rev. B **37**, 9753 (1988).